Available online at www.sciencedirect.com

ScienceDirect

Procedia CIRP 13 (2014) 359 – 364

www.elsevier.com/locate/procedia

2nd CIRP 2nd CIRP Conference on Surface Integrity (CSI)

Development of a metrology workstation for full-aperture and sub-aperture stitching measurements

Christopher W. King[a,*], Matthew Bibby[a,b]

[a]*Zeeko Ltd, Vulcan Court, Coalville LE67 3FW, UK*
[b]*University College London, Gower St, London WC1E 6BT, UK*
* Corresponding author. Tel.: +44-1530-815-832; fax: +44-1530-839-631. *E-mail address*: christopher.king@zeekoresearch.com

Abstract

In this work we examine how stitching interferometry can be used to provide both absolute calibration and also increased spatial resolution for the interferometric measurement of precision surfaces; both are important aspects of precision surface production. We examine the process of stitching as used to form a synthesized full-aperture measurement of a part from sub-aperture data. We then explain how to estimate and remove systematic errors in the interferometer by using the plurality of sub-aperture data sets thereby eliminating the need for a master calibration piece.
We briefly describe our automated stitching system and how it fulfils a specific need in the optics industry to enable high-resolution and calibrated measurements on large aperture optical surfaces. Finally we conclude with some example measurements of real surfaces using the stitching system built at our lab.

Keywords: Interferometry; Calibration; Optical; Optimization

1. Introduction: interferometry and optical form measurements

We describe the motivation for the work by beginning with a very brief overview of the problems addressed, before a brief summary of optical form testing. We then describe a new system to solve the problems before completing our concluding remarks.

A common and increasingly major problem encountered in optical testing laboratories is: *how can one measure the shape, or form, of large diameter plano or convex surfaces where D>100 – 150 mm?* Traditionally this has been very difficult where accuracies of the order of < 200 nm PV are required. Most interferometers do not have a large enough entrance aperture to measure such parts.

A second problem that arises is that of 'absolute calibration'; usually optical surfaces will be compared to a master surface. What is often required is to measure a part to an accuracy better than that of the master surface, if a master surface even exists for the size of the part contemplated.

A third issue is that optical surface forms must often now be measured with increased spatial/lateral resolution in order to extend the measurement of form to overlap with the measurement of waviness or texture.

We describe our solution to these issues in the form of an automated stitching workstation for large parts that simultaneously addresses these issues whilst eliminating some of the measurement burden from the metrologist.

Optical Fizeau interferometry is the standard for high accuracy optical surface form measurements [1]. In Figure 1 monochromatic coherent laser light from a point source/spatial filter is focused into plane wavefronts by lens 'B'. Part 'C' is a removable reference element fixed to the interferometer usually referred to as a Transmission Flat (T/F), or for spherical surfaces, a transmission sphere (T/S). At the rightmost surface of 'C', the light undergoes both reflection and transmission. Provided that the rightmost surface of 'C' is perpendicular to the optical axis, the reflected light will

doi:10.1016/j.procir.2014.04.061

simply retrace its path back into the interferometer via lens ‘B’.

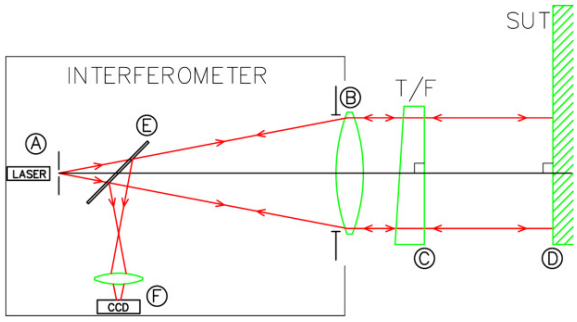

Figure 1. Basic schematic of a Fizeau interferometer.

The transmitted portion of the light from ‘C’ continues until mirror ‘D’. If the surface of ‘D’ is made on average perpendicular to the optical axis, the light will reflect back down the path it came and retrace back into the interferometer. The two light beams, once inside the interferometer (left of lens ‘B’) will interfere. The resulting interference fringe pattern is recorded by the CCD, ‘F’, and processed in a computer to give a height map of the difference between the surfaces ‘C’ and ‘D’ [2]. Key points are:

1. The light beams incident upon the surface under test ‘D’ and the reference surface ‘C’ are at or near normal incidence – the surfaces share a conjugate, finite or infinite.
2. The light source must have a long enough coherence length.
3. The test surface ‘D’ is effectively compared to the reference surface ‘C’, therefore the form errors in ‘C’ must be very small compared to those of ‘D’.

Commercial Fizeau interferometers are common and the art is well established; standard reference elements for 100 and 150 mm diameter systems are available off-the-shelf for testing plane and spherical surfaces. Figure 2 shows a Fizeau configuration for the measurement of spherical convex surfaces – the most problematic types. The lens elements to the left of surface ‘C’, the reference surface, serve to converge the light beam and provide a spherical reference wavefront whose focus lies at the centre of curvature of surface ‘C’. Test surface ‘D’ also has its centre of curvature located at the focus of the test beam maintaining the normal incidence criterion giving rise to the interference.

In general the surface at ‘C’ will have a form accuracy of the order of λ/20 peak-to-valley (PV), where λ is usually 632.8 nm. Therefore, without calibration, the best measurement accuracy that can be achieved will be limited to this value. Stitching systems have been produced before, but not with the extended capability of this system [3].

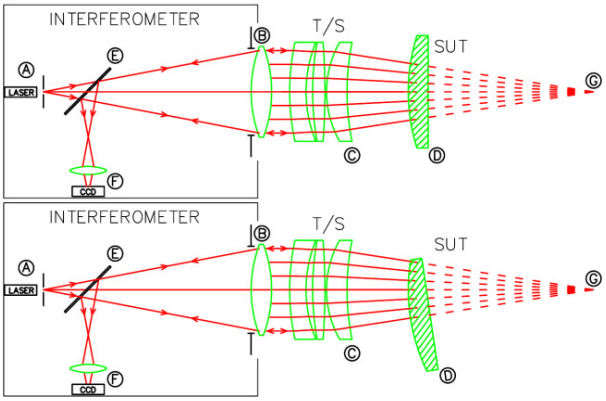

Figure 2. Upper: Fizeau interferometer for testing spherical surfaces. The additional lens elements between ‘B’ and ‘C’ serve to focus the light to a point ‘G’. Light exits the interferometer normal to surface ‘C’. The part ‘D’ has its centre of curvature common with surface ‘C’ preserving autocollimation. Red rays show the extent of the test beam on the part. Lower: Part ‘D’ is rotated about the confocal point ‘G’ to access a different sub-aperture.

1.1. The scope of the work

This work addresses the problem illustrated in Figure 1 and Figure 2 where the interferometer’s beam is simply not large enough to completely measure the surface ‘D’ in the figures. This is a common problem for large diameter plano and convex optical surfaces [4].

This work also addresses the problem of the quality of the reference surface – the surface ‘C’ in the figures. We explain how we can compute the shape of the reference surface using our system to remove systematic measurement errors.

The stitching process described naturally gives an increase in lateral resolution because the interferometer’s sampling elements are spread over a smaller area of the surface under test.

1.2. Commercial system capabilities

This new work builds on and developed at Zeeko and UCL to produce a fully automated stitching workstation that can be used to measure large parts that exceed 500 mm in diameter, many of which cannot be measured by any previous commercial systems. The authors are not currently aware of any system able to achieve this. The system is capable of measuring plane parts, convex and concave spheres, and certain aspheres via a Computer Generated Hologram (CGH) null. The turnkey system includes automated hardware and software tools to make automated measurements. A picture of the completed system is shown in Figure 3.

Figure 3. The Zeeko Stitching Interferometry workstation.

The system finds use in the corrective polishing of ultra-precision optical components for the optics and precision metrology industries.

2. Stitching Interferometry

The principle of stitching is simple: when the whole of a surface cannot be measured in a single go, multiple measurements of smaller portions of the surface are made where there is some degree of overlap between adjacent measurements. These sub-aperture measurements are then processed in a computer algorithm to assemble a synthetic full-aperture measurement. Example stitched data is shown in Figure 4.

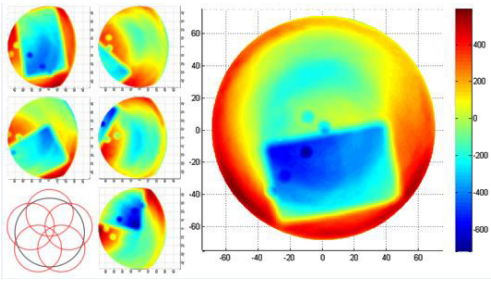

Figure 4. Example sub-aperture data and a resultant stitched full-aperture map showing height deviation as a function of X-Y position. The circles in the lower left relate the part (black) to the sub-aperture positions(red), this is known as the sub-aperture map.

The measurements' centre positions must be made in a known coordinate frame, or there must be some means to perform lateral or pixel registration before piston, tilt (plane) and other polynomial terms can be optimized out. The terms arise owing to small alignment errors between surfaces 'C' and 'D.

As the part is translated and rotated underneath the interferometer small changes in piston, tilt and defocus measurement terms will occur owing to mechanical imperfections of the system used to hold the part and interferometer. The stitcher optimizes these terms once the initial geometric data registration (X-Y) has taken place.

Referring again to Figure 2, the two portions of the figure show the part in two of infinitely many possible relationships to the interferometer. To measure the entire surface, a finite scheme of measurement positions must be chosen that gives the required overlap and provides 100% coverage. To actually measure and move the part requires that the part (or interferometer) is rotated about point 'G' in Figure 2 to maintain the confocal or concentric condition. Using a real world CNC system, this will usually require compound motion in at least 6 high-precision axes for fine nulling of the interference fringes.

3. Stitching Process

The Zeeko Stitching Toolkit uses a custom stitching algorithm based on several key parts that has been developed from collaborative work with UCL:

1. A preprocessor to translate the sub-aperture data into the correct coordinates.
2. The interferometer systematic errors are measured or estimated and then subtracted from each sub-aperture measurement – the 'calibration'.
3. The stitching processor to optimize, power, tilt and other user definable polynomial terms between **overlapping** sub-apertures. The processor provides simultaneous optimization of each sub-aperture to minimize the residuals in the overlap areas between sub-apertures.
4. Output and analysis routines for exporting the measurement data for feedback into corrective polishing processes using multi-axis CNC polishing machinery.

The software operates on all the measured sub-aperture and mechanical configuration data provided by the automated measurement platform.

4. Reference Calibration

Calibration of the interferometer systematic errors is generally necessary when stitching measurements are used.

A typical calibration could involve making a series of measurements over the test surface in multiple positions:

1. To be averaged if the test surface errors are positionally uncorrelated in each measurement. The average of the measurements will converge to the interferometer's reference error when the number of measurements is large enough [5].
2. To be analyzed mathematically to try to solve for either the test or reference surface errors. The most

common method applicable to spheres is attributable to Jensen and is known as the 3-sphere test [6].

The method used in this work involves modelling all the measured data by a set of polynomials and associated coefficients, and estimating the coefficients from the real data and the model, fully taking advantage of the automatic measurements.

4.1. Calibration method: removing systematic errors

The automated stitching gives multiple sub-aperture measurements. Each measurement is a sum of the part's errors, the interferometer's systematic errors and also the alignment terms and noise. We model the real measured data by a sum of orthogonal polynomial functions and the associated polynomial coefficients. We compute the polynomial coefficients that make the model a least-squares fit to the real data, and hence provide a polynomial fit to the interferometer systematic errors.

Generally we use 3 distinct sets of circular Zernike polynomials and associated coefficients for:

1. The shape of the interferometer's systematic errors.
2. The shape of the surface under test.
3. The stitching terms – the piston, tilt and power terms to stitch the data after initial coordinate registration.

Let the all the measured data in N sub-apertures be denoted by, $\boldsymbol{D}$, and let the k^{th} Zernike polynomial in the expansions of the test and reference surfaces be denoted by Z^T_k and Z^R_k respectively. Let $Z^A_{m,l}$ denote the l^{th} Zernike polynomial in the expansion of the alignment terms for the m^{th} sub-aperture. Let a_k, b_k and $c_{m,l}$ denote the coefficients for each of the test surface, interferometer error and alignment polynomials respectively. In a simplistic view we then have our model for the measured data, ignoring for the present the software data ordering and masking issues:

$$D(x,y)=\sum_{k=1}^{j} a_k Z^T_k(x,y)+\sum_{k=1}^{j} b_k Z^R_k(x,y)+\sum_{m=1}^{N}\sum_{l=1}^{\{3,4\}} c_{m,l} Z^A_{m,l}(x,y)$$

In order to solve for the coefficients a_k, b_k and $c_{l,m}$ we take the measured data, $D(x,y)$, and precompute the Zernike basis polynomials on (x,y) to reduce the problem to finding $\boldsymbol{w}$ to minimize the expression $|D-Mw|^2$, where, $\boldsymbol{D}$, is the vector of all measured surface height values taken in a given order, $\boldsymbol{M}$, is the matrix containing the basis Zernike polynomials evaluated in the appropriate ordering on the sub-aperture coordinates, and, $\boldsymbol{w}$, is the unknown vector of all polynomial coefficients. Further processing then discards ambiguous polynomial forms. Once the coefficients, $\boldsymbol{w}$, are known the systematic errors are reconstructed by summing the $b_k*Z^R_k$ polynomial terms. The resulting data map is used to calibrate each sub-aperture.

5. Hardware

The hardware system built [7] can automatically measure sub-apertures on plane, spherical and some aspherical surfaces. The system generates all measurement data for the stitching including a description of all the transformations to be applied on each sub-aperture. The hardware components are:

1. 150 mm aperture phase-shifting interferometer.
2. 5-axis CNC controlled stage for the interferometer providing 3-axes of orthogonal linear motion and two orthogonal tilt axes.
3. Part-holding rotary tilting table with 7 adjustable axes, 3 of which are CNC controlled.
4. Control computer with control and stitching software.

A picture of the working parts of the system is shown in Figure 5.

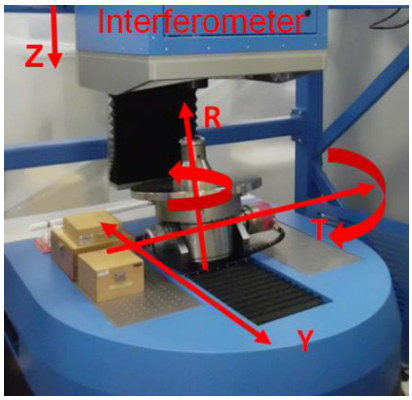

Figure 5. Main visible axes of the automated stitching system.

The custom 8-axis CNC system and axes allow any sub-aperture to be measured on the surface of an f/0.7 sphere up to a maximum diameter of approximately 500 mm whilst keeping the part and interferometer reference surface in the required confocal position for measurements.

The system is controlled via our commercial software application centred on the design of the part to be measured and the selection of the interferometer T/S or T/F. Once a compatible T/S is chosen for the part a sub-aperture layout can be designed to provide enough coverage and overlap to fully measure the SUT.

The part to be measured is mounted onto the rotary table and centred manually. The software system is used to perform:

1. Fine optical clocking (via autocollimation).
2. Determination of the radius of curvature.
3. Determination of the position of the starting sub-aperture.

After part mounting and sub-aperture definition, the measurement proceeds automatically with the system performing the automatic fringe nulling for each sub-aperture.

6. Example measurement results

To demonstrate the accuracy and extended lateral resolution of the system the central 58 mm of a 110 mm diameter convex sphere with a radius of curvature of 87 mm was measured. This was chosen so that we could compare a stitched measurement with a full-aperture measurement. The results are given by PVr [8] and RMS values.

6.1. Convex sphere comparison

An f/3.3 T/S was used for the sub-aperture measurements giving a sub-aperture diameter of 26.3 mm (RoC/f#). A scheme of 25 sub-apertures was used to provide 100% coverage of the central 58 mm diameter region with an adequate inter sub-aperture overlap. The central 58 mm region was the largest diameter that we could measure full-aperture using an f/1.5 T/S (87/1.5 = 58 mm). A typical overlap map is shown in Figure 6.

The interferometer systematic error map was estimated by the algorithm described using a ring of 12 sub-apertures (the software is currently limited to any ring of sub-apertures on a set Pitch Circle Diameter (PCD) from the centre of the SUT). A polynomial fit to the systematic errors was computed using $j=79$ terms. The results of the interferometer systematic error map estimation are shown alongside a conventional 3-sphere computation for comparison in Figure 7.

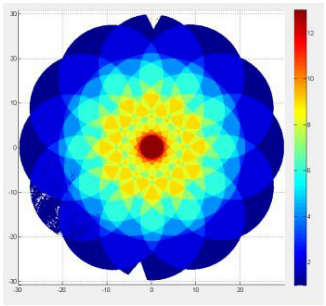

Figure 6. Overlap map for the measurement. The colour scale indicates the number of sub-aperture pixels available at each measurement location.

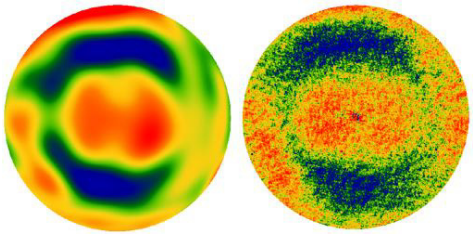

Figure 7. Left: software computed reference surface errors. PVr is 24.0 nm and RMS is 3.7 nm. Right: 3-sphere measured reference surface errors. PVr is 27 nm and RMS is 5.0 nm.

The low-order form comparison is very good the major difference being diffraction and ghosting causing noise in the 3-sphere result.

The part had been fiducialized with reference marks such that the full-aperture map could be registered with the stitched map, and a subtraction made for comparison. The stitched and full-aperture data are shown in Figure 8, whilst the difference map is shown in Figure 9.

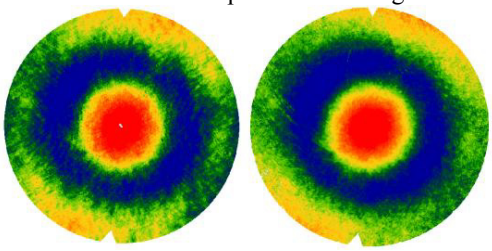

Figure 8. Left: full-aperture result. PVr = 67.3 nm and RMS = 11.3 nm. Right: stitched result. PVr = 68.7 nm and RMS = 11.6 nm.

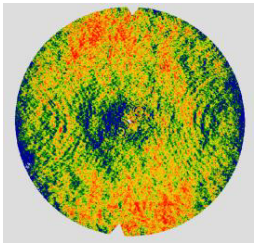

Figure 9. Difference measurement. PVr is 17.7 nm and RMS is 2.9 nm.

The difference shows a PVr of 17.7 nm where most of the remaining form is astigmatism and probably results from two sources:

1. Slight mis-registration errors when subtracting error maps.
2. Long-term thermal changes in the shape of the interferometer reference surface owing to a non-temp stabilized lab.

The results show very good agreement given the poor environment with 3 degrees of temperature variation over a few hours, and λ/37 PVr represents an improvement over the λ/10 reference optics that were used giving credence to the systematic error estimation.

The repeatability of the measurement was also established by taking 10 separate stitched measurements.

The repeatability was calculated as the mean + 2σ of the delta RMS values from the averaged measurement at 1.2 nm. This repeatability should give confidence to optical metrologists.

6.2. Lateral resolution increase

The full-aperture measurement reported in the previous section has a pixel resolution of 90 um/pixel. This contrasts to the 40 um/pixel of the stitched

measurement – an increase in resolution of almost X2.2. This factor can be computed as the ratio of the f-numbers of the transmission spheres used (3.3/1.5 = 2.2). The implications of this are important in the PSD analysis where the full aperture test has a Nyquist limit is at a spatial dimension of 360 um, whereas the stitched measurement extends the spatial frequency response down to 180 um.

This increase in lateral resolution capability can be used to plug the gap between conventional full-aperture interferometry and surface texture measurement using scanning interference microscopes where the upper cut-off can vary from 1 mm down to 0.1 mm depending on the objective used.

Modern sub-aperture precision polishing processes may have raster track spacings of the order of 0.1 – 2 mm and it is therefore important to be able to measure down to slightly higher spatial frequencies. Sub-aperture stitching's enhanced lateral resolution can be used to provide increased resolution form measurement to give enhanced PSD coverage. This allows the impact of the polisher's track spacing on the part's structure to be quantified further down into the crucial mid-spatial frequency regimes.

6.3. Extended aperture capability

A 300 mm diameter convex test-plate was measured with a radius of curvature of 465 mm to demonstrate the extended aperture capability. Normally, on the 6" interferometer used in this system, the maximum diameter of this surface that can be measured is 133 mm using a 150 mm diameter f/3.5 T/S. Since we did not have such a T/S available, we used a 150 mm diameter f/5.4 T/S giving a sub-aperture diameter of 86 mm. The part was measured 3 times in 41 sub-apertures in a lab with 1 degree C temperature control. The averaged measurement result is shown in Figure 10.

We established the repeatability of the test in the same manner as earlier as 1.45 nm. At present, we cannot verify the actual form of the part using another interferometer because we do not have access to one large enough able to measure this part. However, given the good measurement repeatability, we expect that the measurement will be accurate on the order of λ/15 PV in the absence of part deformation and thermal effects given the relatively high-aspect ratio of the part.

7. Conclusion

A new automated interferometry stitching workstation has been demonstrated that is capable of handling large diameter parts which can provide calibrated and automated measurements of several types of surfaces with accuracies that can approach λ/40 PVr.

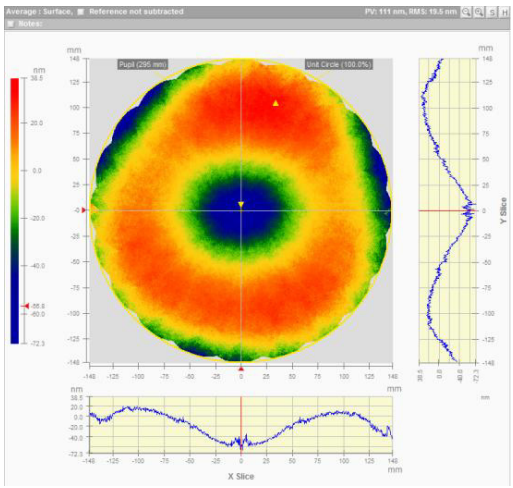

Figure 10. Averaged stitched measurement of the 300 mm diameter convex sphere of radius 465 mm. The PVr is 95.7 nm and the RMS is 19.4 nm.

We are certain that for some parts we can obtain accuracies better than lambda/60 PV under stable conditions with smaller diameter convex parts.

The system has also been shown to have a gain in the spatial resolution available over full-aperture measurements thereby extending the spatial frequency information available to polishers and polishing process developers. The system has also shown to be able to make repeatable measurements on large spherical surfaces up to at least 300 mm in diameter. We hope to be able to report on further work on larger surfaces in the near future.

References

[1] Malacara, D., Ed., 2007. Optical Shop Testing, 3rd ed, wiley, p17.
[2] Malacara, D., Servin, M., Malacara, Z., 2005. Interferogram analysis for optical testing, 2nd ed. Taylor and Francis, ch6.
[3] Tricard, M., Dumas, P., Forbes, G., DeMarco, M., 2006. Recent advances in sub-aperture approaches to finishing and metrology, Proc. SPIE 6149, 614903.
[4] Otsubo, M., Okada, K., Tsujiuchi, J., 1994. Measurement of large plane surface shapes by connecting small-sperture interferograms, Optical engineering, Feb 1994, vol 33(2).
[5] Parks, R., Evans, C., Shao, L., 1998. Calibration of interferometer transmission spheres, Optical fabrication and testing workshop, OSA Technical digest series 12, p80 – 83.
[6] Jensen, A., 1973. Absolute calibration method for Twyman-Green wavefront testing interferometers, J. Opt. Soc. Am. 63, 1313A.
[7] King, C., Bibby, M., 2013. Development of a metrology workstation for full-aperture and sub-aperture stitching measurements, JSPE, International symposium on application of precision engineering to support the next generation astronomical telescopes, Proc JSPE March 2013.
[8] Evans, C., 2009. PVr - – robust amplitude parameter for optical surface specification, Optical Engineering, April 2009, vol 48(4).